

Open Loop Control of The Z Source Resonant Converter for the Electric Vehicle Wireless Battery Charger

Shwetha K B

P.G. Student, Power Electronics,
Dayananda Sagar College of Engg., Bangalore, India,
2014shwethaks@gmail.com

Shubha kulkarni

Asst prof, Electrical & Electronics Engineering
Dayananda Sagar College of Engg., Bangalore, India,
Smk.1978@gmail.com

Abstract— Wireless charger for Electric Vehicles (EVs) is an off-line application and it needs power factor correction (PFC) function, which usually consists of a front-end boost PFC and a cascaded DC/DC converter. Recently, Z-source resonant converter (ZSRC), a single-stage solution with low cost and high efficiency, was proposed for EV wireless charger. Combining with the Z-source network, the control scheme is more challenged and sophisticated. The experimental setup is done for the open loop control of the z source resonant converter. The pic microcontroller is used for the generating the pulse gate for the MOSFET and the conductor coils are used for the wireless power transmission, The experiment is done for the 33v input dc and the 88v dc output voltage prototype.

Keywords:— Closed loop control, Electric vehicle, PI controller, wireless power transfer(WPT), Z source resonant converter(ZSRC).

I. INTRODUCTION

Wireless power transfer(WPT) is emerging as a flexible, convenient, safe, and autonomous charging method for plug-in electric vehicles. WPT's safety stems beyond the inherent isolation between the large between the grid side transmit pad and the vehicle mounted receiver coil.(1) Wireless charging can also be done during inclement weather without being affected from snow or rain without needing bulky cables and heavy duty plugs. The convenience and flexibility of the WPT is not only because no cables and connectors are necessary but due more to the fact that charging becomes fully autonomous.(2) A vehicle to infrastructure (V2I) communications can be implemented to add to the autonomy benefit by handling all the bidirectional communications needed for charging transactions as well as providing the feedback channel for power flow regulation.(3)

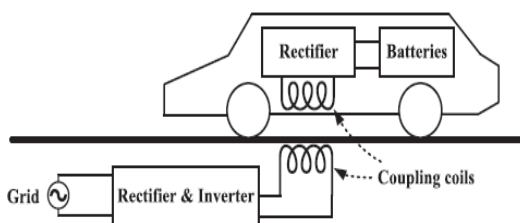


Fig 1. Configuration of a WPT system for on line power transfer(OLPT)

The block diagram of the experimental setup module of the z source resonant converter is shown in fig1. from that the 5v dc is supplied to the PWM controller and the 12v dc is supplied to the MOSFET driver circuit from the step down transformers. The regulated power supply of 0-32v dc is used to supply the z source resonant converter.(4)

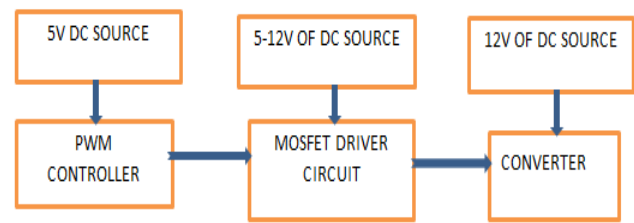


Fig:2 Block diagram of the hardware model of the z source resonant converter for the WPT

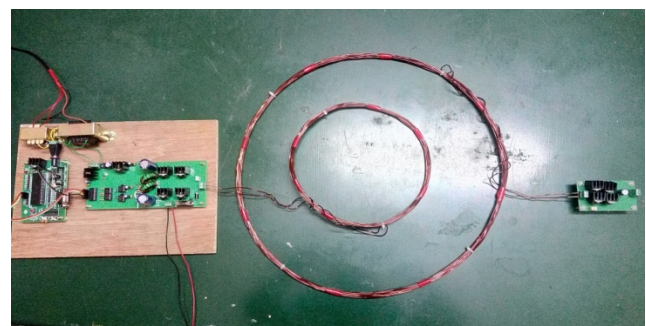


Fig 3 Experimental set up of the z source resonant converter

The pic microcontroller PIC16F882/883/886 is used to generate the gate pulse for the inverter. The input of the microcontroller RB0,RB1,RB2,RB3 is given to the buffer in the MOSFET driver circuit. The Buffers CD4049UB and CD4050B devices are inverting and non-inverting hex buffers, respectively is used to strengthen the signals with no distortions. The ZSRC works on the zero notch control method where in phase-shift control, different phase shifts actually generate different amplitudes of the fundamental component at switching frequency. Thus, controlling a notch width shares a similar idea. Pulse notch control is usually used in a three phase system as it does not damage the symmetry of the three-

phase system. In the case of a single-phase ZSRC, this notch can be either shoot-through state or zero state, Zero state is filled in the middle of active state. Zero notch will help regulating the output power downward..(5)

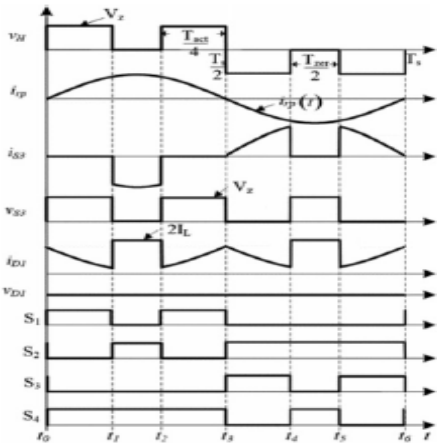


Fig 4 Time domine waveform of the zero notch control

II. DESCRIPTION OF THE COMPONENTS USED IN THE HARDWARE MODEL

Transformers: A Step down Transformer is a type of transformer, which converts a high voltage at the primary side to a low voltage at the secondary side.



Fig 5 Transformer model

2 Pic microcontrollers The PIC16F882/883/886 is available in 28- pin PDIP, SOIC, SSOP and QFN packages. The PIC16F884/887 is available in a 40-pin PDIP and 44- pin QFN and TQFP packages. Figure shows the pin diagram of PIC16F882/88

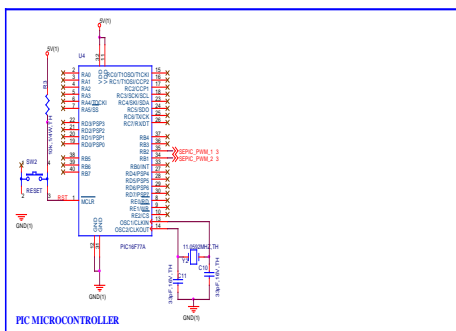


Fig 6 pin diagram of PIC16F882/883/886

3 Buffer: CMOS Hex Buffer/Converters:

The CD4049UB and CD4050B devices are inverting and non-inverting hex buffers, respectively, and feature logiclevel conversion using only one supply voltage (VCC). The input-signal high level (VIH) can exceed the VCC supply voltage when these devices are used for logic-level conversions.

Pinouts

CD4049UB (PDIP, CERDIP, SOIC, SOP, TSSOP)
TOP VIEW

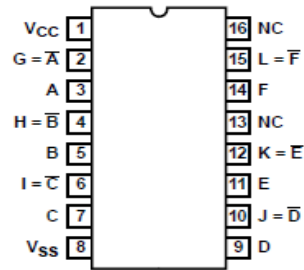


Fig 7 pin diagram of IC CD4049UB and CD4050B

4 Toroidal Inductor: Toroidal inductors and transformers are inductors and transformers which use magnetic cores with toroidal shape. They are passive electronic components consisting of a circular ring or donut shaped magnetic core of ferromagnetic materialsuch as laminated iron,iron powder,or ferrite,around which wire is wounded.

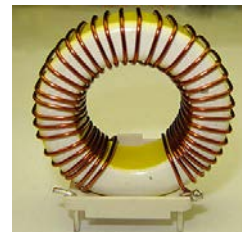


Fig 8 Toroidal inductor

5 MOSFET switch: Third generation Power MOSFETs from Vishay provide the designer with the best combination of fast switching, ruggedized device design, low on-resistance and cost-effectiveness.

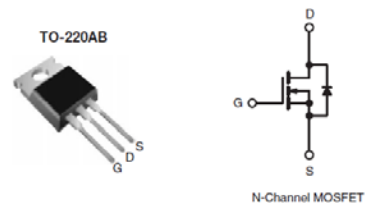


Fig 9 Structure of MOSFET

6 MOSFET DRIVER IC: The IR2101 is a high voltage, high speed power MOSFET and IGBT driver with independent high and low side referenced output channels. Proprietary HVIC and latch immune CMOS technologies enable

ruggedized monolithic construction. The logic input is compatible with standard CMOS or LSTTL outputs.

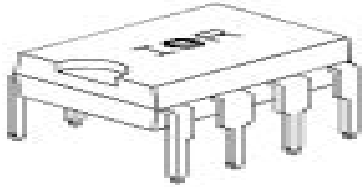


Fig 10 Structure of the MOSFET driver

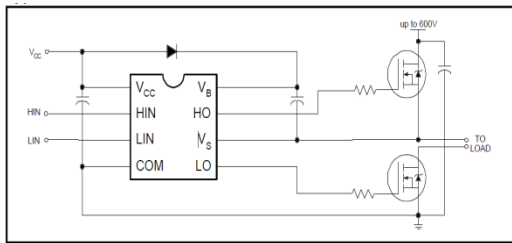


Fig 11 Typical connection of the MOSFET driver

6 Transmitting coils: A typical resonance coupling (MRC) WPT system with four coils is shown. Here, the power transfer between source coil and transmitting coil worked as inductive coupling, between transmitting coil and receiving coil worked as magnetic resonance coupling, and between receiving coil and load coil transfers worked as inductive coupling also.

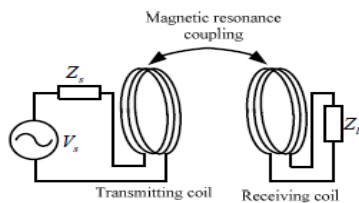


Fig 12 The two coil configuration MRC WPT

III. DESIGNING OF THE Z SOURCE RESONANT CONVERTER

The input voltage of the ZSRC is $V_s=33V$ and the output voltage and current is $V_o=88v$ and $I_o=2.28A$ with the resonant frequency of $20kHz$.(6)

Assuming that the ZSN is symmetrical ($C_1 = C_2 = C$, and $L_1 = L_2 = L$) in Fig. 4, therefore, $V_{C1} = V_{C2} = V_C$, and $V_{L1} = V_{L2} = V_L$. Also, the resonant frequency of L and C in ZSN is at least ten times smaller than the switching frequency. Hence, the ZSN inductor current and the ZSN capacitor voltage are considered constant in one switching cycle. Hence,

$$C_1 = C_2 = C = 4.7mF$$

$$L_1 = L_2 = L = 1mH$$

Assuming purely resistive loading for the converter, then the load resistor can be found as,

$$R_0 = \frac{V_o^2}{P_o} = \frac{88^2}{200} = 38.59\Omega$$

The frequency is selected as $20kHz$. Hence, the period of the circuit is,

$$T_s = \frac{1}{f} = \frac{1}{20k} = 50\mu s$$

The size of the inductors and the average currents through them cannot be determined unless the duty-factor is determined.

$$D = \frac{V_o - V_s}{2V_o - V_s} = \frac{88 - 33}{2 \cdot 88 - 33} = 0.38$$

The output voltage of the z source resonant converter is given by

$$V_0 = \frac{(1-D)V_s}{1-2D} = \frac{(1-0.38)33}{1-2 \cdot 0.38} = 85.25V$$

The output current of the z source resonant converter is given by

$$P = V \cdot I = 85.25 \cdot 2.28 = 194.37W$$

The main requirements of the Z-source dc/dc converter are listed at Table 1.

Input voltage(Vdc)	33V
Output	88 V/2.28A
Resonant frequency	18.2kHz
Transformer turns ratio	15:20
ZSN capacitors(C_1, C_2)	4.7mF
ZSN inductors(L_1, L_2)	1mH
Primary-side compensating capacitor(C_p)	180nF
Primary side leakage inductance(L_{kp})	0.415Mh
Magnetising inductance(L_m)	61.87uH
Secondary side leakage inductance(L_{ks})	1.07Mh
Secondary-side compensating capacitor(C_s)	65.8nF
Output filter capacitor(C_o)	1mF

Table 1. Parameters and values

IV. EXPERIMENTAL RESULTS

Experiment have been performed to validate the previous simulations and analysis of the open loop control of the z source resonant converter. The analysis and the design of the proposed ZSRC system are verified based on the 33v dc input

and 88v output prototype. The parameter of the converter is given in the table 1.(7)

The gate pulse of the MOSFET switches is shown in the below figure

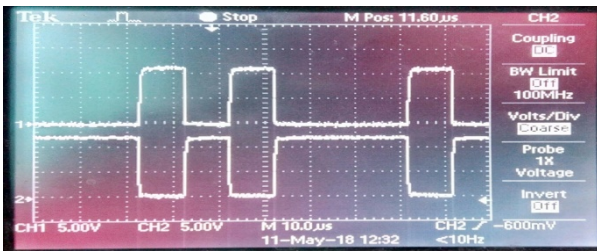


Fig 13 The gate pulse waveform of the MOSFET switches s2 and s1 with the 50% duty cycle.

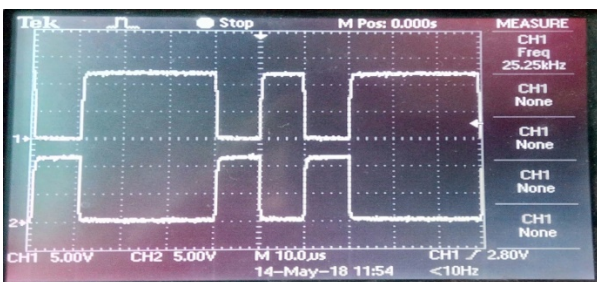


Fig 14 The gate pulse waveform of the MOSFET switches s4 and s3 with 50% duty cycle

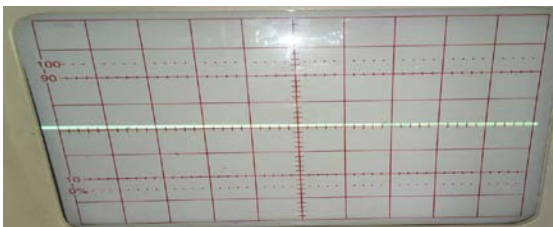


Fig 15 DC output voltage of 72V for 33v of input voltage

V. CONCLUSION

Z-source resonant converter (ZSRC), a single-stage solution with low cost and high efficiency, was proposed for EV wireless charger. The experimental setup is done for the open loop control of the z source resonant converter. The pic microcontroller is used for the generating the pulse gate for the MOSFET and the conductor coils are used for the wireless power transmission, The experiment is done for the 33v input dc and the 88v dc output voltage prototype for no load. The pulse gate and the readings for the various input without load is shown

REFERENCES

[1] S. Y. Choi, B. W. Gu, S. Y. Jeong, and C. T. Rim, "Advances in wireless power transfer systems for roadway-powered electric vehicles," *IEEE J. Emerg. Sel. Topics Power Electron.*, vol. 3, no. 1, pp. 18–36, Mar. 2015.

[2] H. Zeng, S. Yang, and F. Peng, "Wireless power transfer via harmonic current for electric vehicles application," in *Proc. IEEE Appl. Power Electron. Conf. Expo.*, Mar. 15–19, 2015, pp. 592–596.

[3] M. Kwon, S. Jung, and S. Choi, "A high efficiency bi-directional EV charger with seamless mode transfer for V2G and V2H application," in *Proc. 2015 IEEE Energy Convers. Congr. Expo.*, Montreal, QC, Canada, 2015, pp. 5394–5399.

[4] S. Kiratipongvoot, Z. Yang, C. K. Lee, and S. S. Ho, "Design a high frequency-fed unity power-factor AC-DC power converter for wireless power transfer application," in *Proc. 2015 IEEE Energy Convers. Congr. Expo.*, Montreal, QC, Canada, 2015, pp. 599–606.

[5] J. Deng, F. Lu, L. Siqi T.-D. Nguyen, and C. Mi, "Development of a high efficiency primary side controlled 7 Kw wireless power charger," in *Proc. 2014 IEEE Int. Elect. Veh. Conf.*, Dec. 17–19, 2014, pp. 1–6.

[6] S. C. Moon, B.-C. Kim, S.-Y. Cho, C.-H. Ahn, and G.-W. Moon, "Analysis and design of a wireless power transfer system with an intermediate coil for high efficiency," *IEEE Trans. Ind. Electron.*, vol. 61, no. 11, pp. 5861–5870, Nov. 2014.

[7] H. Ishihara et al., "A voltage ratio-based efficiency control method for 3 kW wireless power transmission," in *Proc. 29th Annu. IEEE Appl. Power Electron. Conf. Expo.*, 2014, Mar. 16–20, 2014, pp. 1312–1316.